

Thermomechanical modelling for industrial applications

Nirav Vasant Shah, Michele Girfoglio and Gianluigi Rozza

Abstract In this work we briefly present a thermomechanical model that could serve as starting point for industrial applications. We address the non-linearity due to temperature dependence of material properties and heterogeneity due to presence of different materials. Finally a numerical example related to the simplified geometry of blast furnace hearth walls is shown with the aim of assessing the feasibility of the modelling framework.

Keywords: nonlinear thermomechanical model, finite element method, heterogeneous material, blast furnace.

1 Introduction

Thermomechanical models are widely used in many practical applications [1, 2]. We refer to the case of one-way coupling between thermal and mechanical fields, where the temperature can be computed *in advance*, it being independent of the displacement, and used *afterwards* to compute the displacement. Finite Element Method (FEM) [3] is adopted to obtain these fields by solving the weak formulation of the governing equations. FEM based thermomechanical models have been successfully used for the investigation of thermomechanical phenomena arising in blast furnace [4, 5]. In this work, we are going to take a step forward with respect to what done in [5] by considering the temperature dependence of material properties (that introduces a nonlinearity in the thermal model) and presence of different materials (at which one could refer to as heterogeneous material).

Nirav Vasant Shah, Michele Girfoglio, Gianluigi Rozza
Scuola Internazionale Superiore di Studi Avanzati, via Bonomea, 265 - 34136 Trieste ITALY,
e-mail: shah.nirav@sissa.it, michele.girfoglio@sissa.it, gianluigi.rozza@sissa.it

2 Mathematical model

We consider a thermomechanical problem described in the cylindrical coordinate system (r, y, θ) . In many real-world applications the variation of domain geometry as well as loads and heat fluxes with respect to the angular coordinate θ could be neglected. Under such conditions, it is reasonable to apply axisymmetric hypothesis. Then in the absence of source terms the energy and momentum conservation equations in strong formulation endowed with proper boundary conditions referred to a domain ω can be stated as follows:

$$\text{Thermal model : } -\frac{1}{r} \frac{\partial}{\partial r} \left(rk \frac{\partial T}{\partial r} \right) - \frac{\partial}{\partial y} \left(k \frac{\partial T}{\partial y} \right) = 0, \text{ in } \omega,$$

$$\text{Neumann boundary : } (-k(T, x) \nabla T) \cdot \vec{n} = 0 \text{ on } \Gamma_N^T \subset \partial \omega,$$

$$\text{Convection boundary : } (-k(T, x) \nabla T) \cdot \vec{n} = h(T - T_R) \text{ on } \Gamma_R^T \subset \partial \omega.$$

$$\text{Mechanical model : } \frac{\partial \sigma_{rr}}{\partial r} + \frac{\partial \sigma_{ry}}{\partial y} + \frac{\sigma_{rr} - \sigma_{\theta\theta}}{r} = 0, \text{ in } \omega,$$

$$\frac{\partial \sigma_{ry}}{\partial r} + \frac{\partial \sigma_{yy}}{\partial y} + \frac{\sigma_{ry}}{r} = 0, \text{ in } \omega,$$

$$\text{Applied force : } \boldsymbol{\sigma} \vec{n} = \vec{g}, \text{ on } \Gamma_N^u \subset \partial \omega,$$

$$\text{Bilateral frictionless contact : } \vec{u} \cdot \vec{n} = 0, \vec{\sigma}_t = \vec{0}, \text{ on } \Gamma_c^u \subset \partial \omega.$$

The temperature field T and displacement field $\vec{u} = [u_r, u_y]$ are the unknown quantities of interest. Convection coefficient h , temperature T_R and boundary force \vec{g} are specified data. The relevant material properties include thermal conductivity k , Young's modulus E , Poisson's ratio ν and thermal expansion coefficient α . The normal vector \vec{n} is considered to be pointing outwards. The shear stress $\vec{\sigma}_t$ is related to the stress tensor $\boldsymbol{\sigma}$ as,

$$\vec{\sigma}_t = \boldsymbol{\sigma} \vec{n} - \sigma_n \vec{n}, \text{ where } \sigma_n = (\boldsymbol{\sigma} \vec{n}) \cdot \vec{n}.$$

If T_0 is the known reference temperature, axisymmetric stress-strain relationship, in vector notation, can be expressed as,

$$\{\boldsymbol{\sigma}(\vec{u})[T]\} = \mathbf{C}\{\boldsymbol{\varepsilon}(\vec{u})\} - \frac{E}{(1-2\nu)} \alpha(T - T_0)\{\mathbf{I}\},$$

where $\boldsymbol{\varepsilon}$ is the strain tensor, \mathbf{I} is the identity matrix and

$$\mathbf{C} = \frac{E}{(1-2\nu)(1+\nu)} \begin{bmatrix} 1-\nu & \nu & \nu & 0 \\ \nu & 1-\nu & \nu & 0 \\ \nu & \nu & 1-\nu & 0 \\ 0 & 0 & 0 & \frac{1-2\nu}{2} \end{bmatrix}.$$

At the aim to consider a structure constructed using assembly of different materials, we refer to a domain ω divided into different n_{su} non-overlapping subdomains,

$$\omega = \bigcup_{i=1}^{n_{su}} \omega_i, \quad \omega_i \cap \omega_j = \emptyset, \quad i \neq j. \quad (3)$$

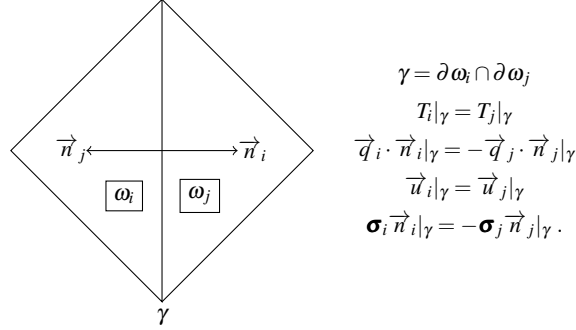


Fig. 1: Close-up view of two subdomains (left) and continuity conditions through the interface between the two subdomains (right).

We refer to the interface between two subdomains $\gamma = \partial\omega_i \cap \partial\omega_j$, $i \neq j$ as shown in Fig. 1 (left). The subdomains ω_i and ω_j are related to different materials. The temperature T and the heat flux $\vec{q} \cdot \vec{n}$, as well as the displacement \vec{u} and the stress vector $\boldsymbol{\sigma} \vec{n}$ are continuous along the interface γ as reported in Fig. 1 (right).

Let $k^{(i)}$, $E^{(i)}$, $\nu^{(i)}$, $\alpha^{(i)}$ respectively be the temperature dependent thermal conductivity, Young's modulus, Poisson's ratio and thermal expansion coefficient corresponding to the material of subdomain ω_i . In the current analysis, we consider $\nu^{(i)}$ and $\alpha^{(i)}$ constant with respect to the temperature. So, for $x \in \omega_i$, we have

$$k(T, x) = k^{(i)}(T), \quad E(T, x) = E^{(i)}(T), \quad \nu(T, x) = \nu^{(i)}, \quad \alpha(T, x) = \alpha^{(i)}.$$

We use the piecewise spline interpolation [6] to approximate thermal conductivity and Young's modulus based on their estimates (typically experimental data) related to certain discrete temperature values:

$$\begin{aligned} \text{if } T_a \leq T \leq T_b, \quad k^{(i)}(T) &= a_{0,k}^{(i)} T^2 + b_{0,k}^{(i)} T + c_{0,k}^{(i)}, \quad E^{(i)}(T) = a_{0,E}^{(i)} T^2 + b_{0,E}^{(i)} T + c_{0,E}^{(i)}, \\ \text{if } T_b \leq T \leq T_c, \quad k^{(i)}(T) &= a_{1,k}^{(i)} T^2 + b_{1,k}^{(i)} T + c_{1,k}^{(i)}, \quad E^{(i)}(T) = a_{1,E}^{(i)} T^2 + b_{1,E}^{(i)} T + c_{1,E}^{(i)}. \end{aligned}$$

We introduce weighted Sobolev spaces, $L_r^2(\omega)$ and $H_r^1(\omega)$ [7]:

$$L_r^2(\omega) = \left\{ \psi : \omega \mapsto \mathbb{R}, \int_{\omega} \psi^2 r dr dy < \infty \right\},$$

$$H_r^1(\omega) = \left\{ \psi : \omega \mapsto \mathbb{R}, \int_{\omega} \left(\psi^2 + \left(\frac{\partial \psi}{\partial r} \right)^2 + \left(\frac{\partial \psi}{\partial y} \right)^2 \right) r dr dy < \infty \right\},$$

and the functional spaces for temperature and displacement:

$$\mathbb{T} = \{ \psi \in L_r^2(\omega) \cap H_r^1(\omega_i) \},$$

$$\mathbb{U} = \{ \vec{\phi} \in [L_r^2(\omega)]^2, \boldsymbol{\varepsilon}(\vec{\phi}) \in [L_r^2(\omega_i)]^{3 \times 3}, \vec{\phi} \cdot \vec{n} = 0 \text{ on } \Gamma_c^u \}.$$

Then the weak formulations corresponding to equations (1) and (2) are given by,

$$\sum_{i=1}^{n_{su}} \int_{\omega_i} k \nabla T : \nabla \psi r dr dy + \int_{\Gamma_R^T} h T \psi r dr dy = \int_{\Gamma_R^T} h T_R \psi r dr dy, \quad \forall \psi \in \mathbb{T}, \quad (4)$$

$$\sum_{i=1}^{n_{su}} \int_{\omega_i} \mathbf{C} \{ \boldsymbol{\varepsilon}(\vec{u}) \} : \{ \boldsymbol{\varepsilon}(\vec{\phi}) \} r dr dy = \sum_{i=1}^{n_{su}} \int_{\omega_i} \mathbf{C}(T - T_0) \boldsymbol{\alpha} \{ \mathbf{I} \} : \{ \boldsymbol{\varepsilon}(\vec{\phi}) \} r dr dy$$

$$+ \int_{\Gamma_N^u} \vec{\phi} \cdot \vec{g} r dr dy, \quad \forall \vec{\phi} \in \mathbb{U}. \quad (5)$$

3 Numerical example

We consider the domain ω as shown in Fig. 2, divided in $n_{su} = 6$ subdomains. At top boundary γ_+ and symmetry boundary $\gamma_s = \partial \omega \cap (r = 0)$, Neumann boundary and bilateral frictionless contact are applied. At bottom boundary γ_- , convection boundary and bilateral frictionless contact are applied. Inner boundary γ_{sf} and outer boundary γ_{out} are convection boundaries with applied force. Table 1 reports thermal conductivity and Young's modulus values used for the interpolation. Table 2¹ shows the interpolation coefficients for thermal conductivity and Young's modulus. For sake of simplicity, we consider thermal conductivities $k^{(3)}, k^{(4)}, k^{(6)}$ and Young's modulus $E^{(6)}$ as constant with respect to temperature. Table 3 reports the Poisson's ratio and thermal expansion coefficient values. We use Lagrange finite element with polynomial of degree 1 for displacement and temperature. The number of degrees of freedom for temperature was 4428 and for displacement was 8856. We use Newton's method to solve the nonlinear thermal model (4) with required residual tolerance of $1e - 4$. For the mechanical model (5), we use the lower-upper (LU) decomposition. We set $h|_{\gamma_{sf}} = 2000 \frac{W}{m^2 K}$, $h|_{\gamma_{out}} = h|_{\gamma_-} = 200 \frac{W}{m^2 K}$, $T_R|_{\gamma_{sf}} = 1773K$, $T_R|_{\gamma_{out}} = T_R|_{\gamma_-} = 300K$, $\vec{g}|_{\gamma_{sf}} = -77106(y_{max} - y) \vec{n} \frac{N}{m^2}$, $\vec{g}|_{\gamma_{out}} = \vec{0} \frac{N}{m^2}$ and $T_0 = 300K$. Numerical results were computed by using FEniCS [8] and are shown in Fig. 3.

¹ The coefficients in Table 2 are rounded-off to maximum two decimal points.

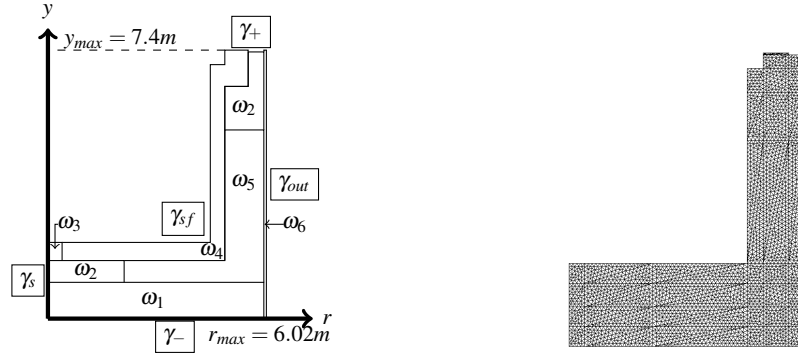


Fig. 2: Computational domain (left) and view of the mesh (right).

$T(K)$	Thermal conductivity ($\frac{W}{mK}$)						$T(K)$	Young's modulus (GPa)					
	ω_1	ω_2	ω_3	ω_4	ω_5	ω_6		ω_1	ω_2	ω_3	ω_4	ω_5	ω_6
293	16.07	49.35	5.3	4.75	23.34	45.6	293	10.5	15.4	58.2	1.85	14.5	190
473	15.53	24.75	5.3	4.75	20.81	45.6	573	10.3	14.7	67.3	1.92	15.0	190
873	15.97	27.06	5.3	4.75	20.99	45.6	1073	10.4	13.8	52.9	1.83	15.3	190
1273	17.23	38.24	5.3	4.75	21.62	45.6	1273	10.3	14.4	51.6	1.85	13.3	190

Table 1: Temperature dependent thermal conductivity and Young's modulus values used for interpolation.

	$a_{0,k}^{(i)}$	$b_{0,k}^{(i)}$	$c_{0,k}^{(i)}$	$a_{1,k}^{(i)}$	$b_{1,k}^{(i)}$	$c_{1,k}^{(i)}$	$a_{0,E}^{(i)}$	$b_{0,E}^{(i)}$	$c_{0,E}^{(i)}$	$a_{1,E}^{(i)}$	$b_{1,E}^{(i)}$	$c_{1,E}^{(i)}$
ω_1	1.4E-5	-1.3E-2	1.9E1	-4.7E-6	1.1E-2	1.1E1	1.2E3	-1.6E6	1.1E10	-1.2E3	2.4E6	9.2E9
ω_2	3.9E-4	-4.3E-1	1.4E2	-1.2E-4	2.5E-1	-8.7E1	-4.5E2	-2.3E6	1.6E10	9.1E3	-1.8E7	2.3E10
ω_3	/	/	5.3	/	/	5.3	-1.05E5	1.2E8	3.1E10	6.1E4	-1.5E8	1.4E11
ω_4	/	/	4.75	/	/	4.75	-7.4E2	8.8E5	1.7E9	6.5E2	-1.4E6	2.6E9
ω_5	3.9E-5	-4.4E-2	3.3E1	-1.3E-5	2.6E-2	9.2	1.3E3	8.9E5	1.4E10	-1.9E4	3.4E7	5.6E8
ω_6	/	/	45.6	/	/	45.6	/	/	1.9E11	/	/	1.9E11

Table 2: Interpolation coefficients for thermal conductivity ($T_a = 293K, T_b = 673K, T_c = 1800K$) and for Young's modulus ($T_a = 293K, T_b = 823K, T_c = 1800K$).

	ω_1	ω_2	ω_3	ω_4	ω_5	ω_6
$\nu^{(i)}$	0.3	0.2	0.1	0.1	0.2	0.3
$\alpha^{(i)}(K^{-1})$	2.3E-6	4.6E-6	4.7E-6	4.6E-6	6E-6	1.2E-5

Table 3: Poisson's ratio and thermal expansion coefficient values.

4 Concluding remarks

In this work we have addressed the development of a thermomechanical model able to describe phenomena associated to the temperature dependence of material properties (non linearity) and to the presence of different materials (heterogeneity). We

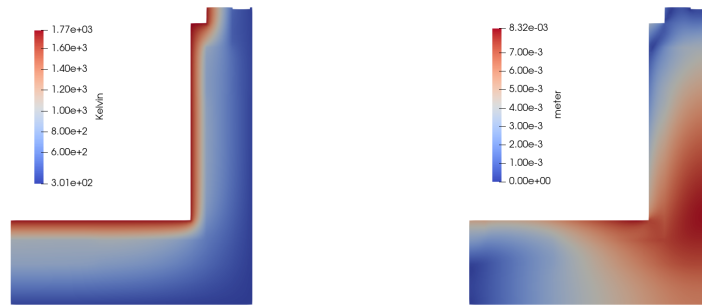


Fig. 3: Computed temperature field (left) and displacement field (right).

expect this preliminary work could serve as starting point for thermomechanical analysis of practical problems.

Acknowledgements We acknowledge the financial support of the European Union under the Marie Skłodowska-Curie Grant Agreement No. 765374 and the partial support by the European Union Funding for Research and Innovation - Horizon 2020 Program - in the framework of European Research Council Executive Agency: Consolidator Grant H2020 ERC CoG 2015 AROMA-CFD project 681447 “Advanced Reduced Order Methods with Applications in Computational Fluid Dynamics”. This work has focused exclusively on civil applications. It is not to be used for any illegal, deceptive, misleading or unethical purpose or in any military applications causing death, personal injury or severe physical or environmental damage.

References

1. Benner P, Herzog R, Lang N, Riedel I, Saak J (2019) Comparison of model order reduction methods for optimal sensor placement for thermo-elastic models. *Engineering Optimization* Volume 51, Issue 3:465–483.
2. Dialami N, Chiumentì M, Cervera M, and Agelet de Saracibar C (2017) Challenges in Thermo-mechanical Analysis of Friction Stir Welding Processes. *Archives of Computational Methods in Engineering* Volume 24:189–225.
3. Brenner S, Scott R, (2008) *The Mathematical Theory of Finite Element Methods*. In: Springer-Verlag New York, 3rd edn.
4. Vázquez-Fernández S, García-Lengomín Pieiga A, Lausín-González C, Quintela P, (2019) Mathematical modelling and numerical simulation of the heat transfer in a trough of a blast furnace. *International Journal of Thermal Sciences* Volume 137:365-374.
5. Shah N V, Girfoglio M, Quintela P, Rozza G, García-Lengomín Pieiga A, Ballarin F, Barral P, Finite element based model order reduction for parametrized one-way coupled steady state linear thermomechanical problems, *In preparation*.
6. Quarteroni A, Sacco R, Saleri F, (2007) *Numerical Mathematics*. In: Springer-Verlag Berlin Heidelberg, 2nd edn.
7. Li H (2011) Finite element analysis for the axisymmetric Laplace operator on polygonal domains. *Journal of Computational and Applied Mathematics* Volume 235, Issue 17:5155-5176.
8. FEniCS Project 2019.1.0, www.fenicsproject.org.